

Prescribed Performance Control Based on PSO Identification and Disturbance Observer for Automotive Electronic Throttle System with Actuator Constraint

Zitao Sun, Xiaohong Jiao, Jiaqi Xue

Institute of Electrical Engineering, Yanshan University, Qinhuangdao, 066004 China (e-mail: jiaoxh@ysu.edu.cn)

Abstract: To further improve the transient and static performance of the practical automotive electric throttle control system against nonlinearity and uncertainty, a prescribed performance-based servo control strategy is investigated in this paper for the electric throttle system with actuator constraint. For handling the uncertain system parameters, particle swarm optimization (PSO) is adopted to identify the nominal physical parameters and disturbance observer technique is utilized to estimate the parameter perturbations and load torque. Moreover, for the practicability of prescribed performance control, the actuator constraint is considered in the controller design. Theoretical analysis is given to prove the tracking performance with the required transient and steady states of the resulting closed-loop system. Meanwhile, the effectiveness and applicability of the proposed control strategy are shown by both Matlab/Simulink simulation and dSPACE-based hardware-in-the-loop experimental verification.

Keywords: electronic throttle system (ETS), actuator constraint, prescribed performance control, particle swarm optimization (PSO), parameter identification

1. INTRODUCTION

As the core part of the automobile engine control system, the electronic throttle control system plays an important role in emissions performance and fuel economy of automobile Cook et al., (2006); Li et al., (2018). However, in the practical electronic throttle system, there exist strongly nonlinear factors including friction, return springs, gear backlash, and parameter uncertainties caused by incomplete system physical parameters and device aging. These factors not only significantly increase the difficulty of the controller design, but also greatly affect the system control performance. Hereby, continuing efforts to improve transient and static performance focus on developing the effective control strategies to restrain the influence of the nonlinearities and uncertainties to fast and accurately tracking the reference command.

Many advanced control strategies are applied in the automotive electronic throttle control systems to achieve fast dynamic response and robust performance against nonlinearities and uncertainties. Various control methods based on the identified system model are proposed, such as, the compound controls of PID feedback and friction compensator adopted in Deur et al., (2004); Pujol et al., (2015), the feedback linearization control methods used in Loh et al., (2007); Grepl and Lee, (2010), and the finite-time convergence control strategy presented in Li and Jiao,

(2017). Meanwhile, some special control methods dealing with the uncertainty are adopted, such as, adaptive, neural network, fuzzy, and sliding mode techniques. Nonlinear adaptive control techniques are utilized to estimate and compensate all uncertain parameters in Pozo et al., (2009); Bernardo et al., (2010); Jiao et al., (2014); Bai, (2018); Jiao et al., (2018) so as to achieve strong robust tracking control performance. Neural networks are utilized in Yuan et al., (2010a,b) to identify the electronic throttle system and to design tracking controller. A recurrent neural network (RNN) identifier and a fuzzy neural network (FNN) controller are presented in Yuan et al., (2010b), and two radial basis function (RBF) neural networks are used in the identifier and the controller in Yuan et al., (2010a). Fuzzy control technique is utilized in Wang and Huang, (2013) to design a fuzzy logic controller. Fuzzy approach are adopted in Sun et al., (2018); Yang et al., (2018) to establish fuzzy model for the uncertainties of the electronic throttle, and then optimal robust controller and the integral sliding mode controller based on this fuzzy model are designed, respectively. Various modified sliding mode control (SMC), integral SMC Li et al., (2017); Wang et al., (2018a), and fast nonsingular SMC Wang et al., (2018b), are employed to design the tracking controllers based on the observers for the uncertainty of electronic throttles.

Nevertheless, for the electronic throttle control system with a crucial requirement for the transient and static performance, a very fast response time and near zero overshoot still are needed to ensure the drivability, fuel economy, and emission performance of the vehicle. Fortunately,

* This work was supported by the National Natural Science Foundation of China (No.61573304) and the Natural Science Foundation of Hebei Province (Grant No.F2017203210).

a particular performance bound technique is presented in Bechlioulis and Rovithakis, (2009); Han and Lee, (2013), which can guarantee that the transient performances of errors converge at the prescribed convergence rate and overshoot. This method has been utilized in many practical applications, such as in servo mechanism Na et al., (2014), robots Psomopoulou et al., (2015); Wang et al., (2017), and vessel Zheng and Feroskhan, (2017).

On the other hand, it should be noted that the more strict control performance is required, the more likely the higher gains of the designed theoretically control input appears. While the designed controller is implemented in practice, this often produces control-signal saturation due to the physical restriction of the actuator. This saturation problem will potentially affect the actual control system resulting in the degradation of the control performance or even the loss of stability if mishandled. In view of the fact, many control strategies dealing with the input saturation have been presented. For example, in view of large high-frequency gains of prediction filters in the minimum-variance controllers, two methods, employing frequency weighting and adaptive scheme iteratively over a finite duration, are presented in Perez-Arancibia et al., (2010) to eliminate the control input saturation problem. Taking saturation into account in the backstepping design of controller, a smooth function is used in Wen et al., (2011) to approximate the saturation with a bounded approximation error, and a Nussbaum function is introduced to compensate for the nonlinear term arising from the input saturation. In Chen et al., (2011), an auxiliary design system is introduced into the adaptive tracking control design to compensate for the effects of input saturation for a class of uncertain multi-input and multi-output nonlinear systems. This method is incorporated in the controller design for various physical systems with the input saturation by Zheng and Feroskhan, (2017); Bai, (2018).

In this paper, the contribution is to apply the prescribed performance control combined with PSO identification and adaptive estimate technique in the actual automobile electronic throttle control system to further improve and guarantee the robust transient and static performance against nonlinearity and uncertainty. Meanwhile, the control input saturation is dealt with by introducing an auxiliary system in the theoretical design of the tracking controller. The remainder of this paper is organized as follows. In Section 2, the electronic throttle system and control mission are briefly introduced. In Section 3, a prescribed performance servo control strategy is designed for a real electronic throttle with the control constraint based on the PSO identification and adaptive estimate of the system physical parameters. The stability and convergence guaranteeing the prescribed performance is analyzed for the closed-loop system with the proposed control strategy. The effectiveness verification and comparative result are presented by both simulation and experimental test in Sections 4. Finally, the conclusion is given in Section 5.

2. ELECTRONIC THROTTLE SYSTEM AND CONTROL MISSION

In this paper, an electronic throttle body used in real cars is selected as the researched object as the same as in Xue et

al., (2018). Its schematic is shown in Fig.1, which includes an accelerator pedal, electronic control unit (ECU) and throttle body comprised of a DC motor, a reduction gear set, a valve plate, reverse springs, and position sensors. The voltage signals of the accelerator pedal sensor and the throttle position sensor are dealt with in the ECU. The control signal generating from the ECU renders the forward and reverse rotation of the DC motor by the duty cycle of the pulse width-modulated (PWM) voltage. The DC motor actuates the throttle valve plate opening by the transmission force of the reduction gear box, the elastic force of the reverse spring and the friction force.

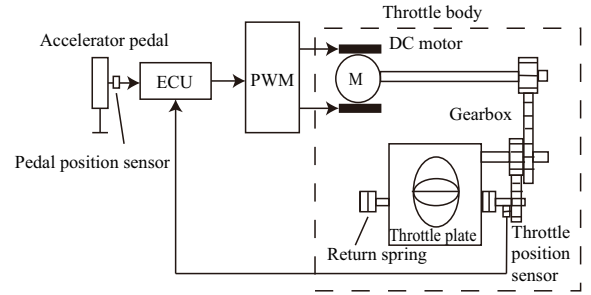


Fig. 1. Schematic of an electronic throttle control system.

According to the electrical and mechanical characteristics of the electronic throttle, the dynamics of the system can be described as follows:

$$u = L \frac{di_a}{dt} + Ri_a + K_e \omega_m \quad (1)$$

$$J_m \dot{\omega}_m = K_t i_a - B_m \omega_m - T_m \quad (2)$$

$$J_t \dot{\omega} = T_l - B_t \omega - T_{sp}(\theta) - T_f(\omega) - T_L \quad (3)$$

where u is the control voltage, ω_m is the motor angular velocity, i_a is the armature current, L and R are the inductance and resistance of the armature circuit, respectively. K_t , K_e are the torque constant and the electromotive force constant of motor, respectively. J_m , B_m and J_t , B_t are the moment inertia and the viscous damping constants of the motor and of the throttle plate, respectively. T_m and T_l are the input and the output torque of the gearbox, respectively. θ and $\omega = \dot{\theta}$ are the opening angle and the angular velocity of the throttle plate, respectively. T_L is the load torque including the disturbance torque caused by the effect of air flow force acting on the throttle plate. T_f is the friction torque, and T_{sp} is the return-spring torque, which are described as follows:

$$T_f(\omega) = F_c \text{sgn}(\omega) \quad (4)$$

$$T_{sp}(\theta) = T_{LH} \text{sgn}(\theta - \theta_0) + K_s(\theta - \theta_0), \theta_{\min} \leq \theta \leq \theta_{\max} \quad (5)$$

where F_c is the coulomb friction coefficient, T_{LH} and K_s are the spring offset and gain, respectively. θ_0 is called limp-home (LH). $\text{sgn}(\cdot)$ is the sign function. Assume that there is no loss during transmission and the backlash is neglected, the gearbox transmission model is $T_l = nT_m$, where n is the gear ratio. Considering the input saturant constraint $-U_{\min} \leq u(t) \leq U_{\max}$, define

$$u(v(t)) = \begin{cases} U_{\max} & \text{if } v(t) > U_{\max} \\ v(t) & \text{if } -U_{\min} \leq v(t) \leq U_{\max} \\ U_{\min} & \text{if } v(t) < -U_{\min} \end{cases} \quad (6)$$

where U_{\min} and U_{\max} are known constants. $u(v(t))$ denotes the plant input subject to saturation type nonlinearity.

In addition, since the value of the armature inductance is small, it can be ignored. For a real electronic throttle, the physical parameters $L, R, K_s, T_{LH}, F_c, J, B, K_t$, and K_e are generally incomplete and have device aging, meanwhile, there is the unknown air flow force disturbance in load torque T_L . The dynamic model of the electronic throttle is simplified to the second-order system:

$$\begin{cases} \dot{\theta} = \omega \\ b\dot{\omega} = u(v(t)) - a_1\theta - a_2\omega + a_3 - a_4\text{sgn}(\theta - \theta_0) \\ - a_5\text{sgn}(\omega) - \bar{T}_L + \Delta(t) \end{cases} \quad (7)$$

where $a_i, (i = 1, \dots, 5), b$ are parameters related to the nominal physical parameters, defined as follows, and \bar{T}_L is related to the load disturbance, $\Delta(t)$ represents the perturbations of the system parameters. $d(t) = \Delta(t) - \bar{T}_L$ can be regarded as an unknown disturbance input.

$$a_1 = \frac{RK_s}{nK_t}, a_2 = \frac{BR + n^2K_tK_e}{nK_t}, a_3 = \frac{RK_s}{nK_t}\theta_0, a_4 = \frac{RT_{LH}}{nK_t},$$

$$a_5 = \frac{RF_c}{nK_t}, b = \frac{JR}{nK_t}, \bar{T}_L = \frac{RT_L}{nK_t}, J = n^2J_m + J_t, B = n^2B_m + B_t.$$

In this paper, the controller is designed based on identification for nominal parameters a_i, b and the estimate for the unknown disturbance input $d(t)$ (Corless and Tu (1998)). Thereafter, for achieving the control objective of the throttle angle θ tracking the desired trajectory θ_r with the required transient and static tracking performance, the prescribed performance control technique is introduced in the tracking controller design to satisfy the following control specifications.

- (1) The adjustment time is required to be less than 100 ms for any operating conditions and reference signal changes, meanwhile, no overshoot should be present in the step response, furthermore, the throttle plate shall never hit the mechanical end stroke Bernardo et al., (2010); Jiao et al., (2014).
- (2) The average value of the steady-state tracking error is not larger than 0.11deg Deur et al., (2004).
- (3) The tracking error response curve $e(t)$ of the system is between the upper and lower limits of the set performance function $\rho(t) = (\rho_0 - \rho_\infty)e^{-\lambda t} + \rho_\infty$ with positive constants defined appropriately ρ_0, ρ_∞ , and λ , furthermore, for no overshoot, the transient response satisfies $0 < e(t) < \rho(t)$ if the initial tracking error is more than 0 and the transient response satisfies $-\rho(t) < e(t) < 0$ if the initial tracking error is less than 0, and the steady-state error of the system are not more than the set parameters ρ_∞ .
- (4) The controller designed should conform to physical constraints on control inputs and safety constraints.

3. PRESCRIBED PERFORMANCE SERVO CONTROL STRATEGY

3.1 System Parameter identification

PSO-based closed-loop identification method is adopted in this paper to identify the system nominal parameters of a real ETS. The schematic diagram of the identification process is shown in Fig.2, where θ_a and θ_i are the actual throttle angle and the throttle angle of the identified model, respectively. θ_r is the reference angle that is a

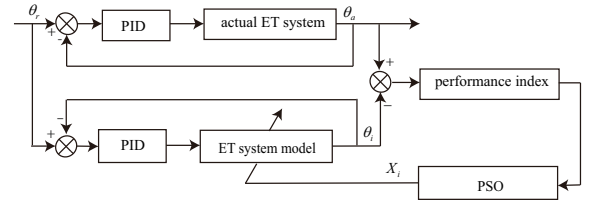


Fig. 2. Schematic diagram of the parameter identification.

set of signals activating the internal characteristics of the ETS. Moreover, the actual ETS is from a hardware-in-the-loop (HIL) platform shown in Fig.3. The PID controller in the identified model system is the same as that in the actual system, and the proportional, integral, derivative coefficients are $k_p = 0.7, k_i = 0.7, k_d = 0.17$, respectively.



Fig. 3. HIL test platform of electronic throttle system.

The fitness function in PSO is chosen as the time weighted squared error integral:

$$ITSE = \int_0^{t_f} t(\theta_a - \theta_i)^2 dt.$$

t_f is the whole running time of a set of excitation signals. $X_i = [X_{i1}, \dots, X_{iD}]^T$ is a vector consisting of $D=9$ parameters identified $L, R, K_s, T_{LH}, F_c, J, B, nK_t, nK_e$, which is regarded as the i th particle in $X = (X_1, X_2, \dots, X_m)$. m is an appropriate number of particles chosen as a swarm X . Each particle X_i is a potential solution of the optimization problem, and the final optimal solution is obtained by the iterative optimization (Kennedy and Eberhart, (1995); Alf, (2011)). During iteratively solving process, the individual extremum $P_i = \{X_i^k | \min\{ITSE\}\}$ in the k th iterative step, and the global extremum $P_g = \{P_i | \min\{ITSE\}\}$. The particle X_i^k in each iterative step is updated according to the following update principle:

$$\begin{cases} X_{id}^{k+1} = X_{id}^k + V_{id}^{k+1}, \\ V_{id}^{k+1} = wV_{id}^k + r_1c_1(P_{id}^k - X_{id}^k) + r_2c_2(P_{gd}^k - X_{id}^k) \end{cases} \quad (8)$$

where $i = 1, 2, \dots, m, d = 1, 2, \dots, D, k = 1, 2, \dots, k_m$. $V_{i1} = [V_{i1}, V_{i2}, \dots, V_{iD}]^T$ is the velocity vector of the i th particle. r_1, r_2 are random numbers distributing on $[0, 1]$. c_1, c_2 are non-negative constants called the acceleration factors, here $c_1 = 2.305, c_2 = 0.195$ (according to $c_1 + c_2 = 2.5$ Alf, (2011); Li and Jiao, (2017)). w is the weighting factor. Considering that a larger w in the early stage of the iteration can expand the search space to improve the global search ability and a smaller w in the late stage can enhance the local search to improve the convergence speed, thus, in this paper, w is chosen as a variable number:

$$w = w_{\min} + (w_{\max} - w_{\min}) * (k_m - k) / k_m \quad (9)$$

where choose $w_{\max} = 0.9, w_{\min} = 0.4, m = 20, k_m = 150$.

Besides, for avoiding the particles into the local optimum, mutation operator is applied to PSO algorithm (Alfi, (2011); Li and Jiao, (2017)). The procedure of PSO-based parameter identification is described in detail as follows:

i. Initialization step: initialize X_i^0 , V_i^0 , and $P_i = X_i^0$, $P_g = \{P_i | \min\{ITSE\}, i \in (1, 2, \dots, m)\}$.

ii. Iteration step: update X_i^k, V_i^k by (8), compute P_i, P_g .

iii. Mutation step: if P_g maintains the same value for 5 iterations in the iterative process and the criterion not within the allowable error ϵ_0 , here $\epsilon_0 = 10^{-4}$, then initializing randomly the particles P_g with a probability of 10% through the roulette selection.

iv. Judgment step: if $P_g \geq \epsilon_0$, then goto step ii, and if $k < k_m$ goto step ii.

v. Output step: output the optimal $P_g^* = ITSE_{\min} \rightarrow [L, R, K_s, T_{LH}, F_c, J, B, nK_t, nK_e]^T$.

Accordingly, the fitness value in the identification iteration is shown in Fig.4. The identified parameters are listed in Table 1. It should be mentioned that the "limping home" angle θ_0 can be obtained by measuring the position of throttle valve plate in the static state.

Table 1. System parameters identified

Parameters	Value	Unit
J	0.0018	kgm ²
B	0.0056	Nm/rad/s
nK_t	0.5331	Nm/A
nK_e	0.6420	V/rad/s
k_s	0.0885	Nm/rad
T_{LH}	0.4418	Nm
F_c	0.2111	Nm
R	1.6057	Ω
L	0.0052	H

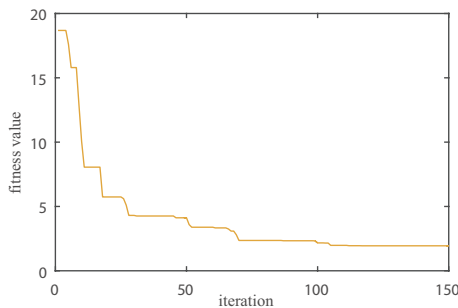


Fig. 4. Fitness value in the identification iteration.

Fig. 5. Validation of the parameter identification.

The identification effectiveness is validated in the test platform of Fig.3. The validation result is shown in Fig.5, which is the comparison between the output of the model with the identified parameters and the actual system output when imposing the same reference input. It shows the synchronization of the output of the PSO-based identification model with the output of the actual system within certain limited error, which means that the identified model is useful to the model-based controller design.

3.2 Identification-based prescribed performance controller

Based on the PSO identification result, the prescribed performance control technique is utilized to design a servo control strategy for the electronic throttle system.

Accordingly, for the system (7) with the identified parameters, a prescribed performance servo controller with the estimate of the unknown disturbance input is designed as:

$$v(t) = b\ddot{\theta}_r + a_1\theta + a_2\omega - a_3 + a_4\text{sgn}(\theta - \theta_0) + a_5\text{sgn}(\omega) - \hat{d}(t) - b\dot{\alpha} + \xi(t)/\varphi(t) + k_2z + k_3(z - \eta) \quad (10)$$

according to Corless and Tu (1998) and noting that the nominal value of $d(t)$ is zero, $\hat{d}(t)$ is constructed as:

$$\begin{cases} b\dot{\hat{d}} = u - a_1\theta - a_2\omega + a_3 - a_4\text{sgn}(\theta - \theta_0) - a_5\text{sgn}(\omega) + \hat{d} \\ \hat{d}(t) = \gamma b(\omega - \hat{\omega}), \gamma > 0 \end{cases} \quad (11)$$

the virtual control law

$$\alpha = (\dot{\varphi} - k_1\varphi)\xi, \quad z = \dot{\theta}_r - \omega - \alpha \quad (12)$$

the transformation of error

$$\xi(t) = e(t)/\varphi(t), \quad e(t) = \theta_r - \theta \quad (13)$$

$\varphi(t)$ is a piecewise continuous function defined as the following form, which is related to the tracking error $e(t)$:

$$\varphi(t) = \begin{cases} \rho(t), & e(t) \geq 0 \\ -\rho(t), & e(t) < 0 \end{cases} \quad (14)$$

and the auxiliary design system used to reduce the saturation effect Bai, (2018):

$$\dot{\eta} = \begin{cases} -k_4\eta - \frac{|zN(v-u)| + 0.5(v-u)^2}{\eta^2}\eta + (v-u), & |\eta| \geq \varepsilon \\ 0, & |\eta| < \varepsilon \end{cases} \quad (15)$$

where ε is a small positive design parameter. $k_i, (i = 1, \dots, 4)$ are positive adjustable parameters satisfying

$$k_2 + 0.5k_3 > 0, \quad k_4 > 0.5(1 + k_3), \quad N > 1 \quad (16)$$

It should be noted that $\dot{\varphi}(t)$ exists when the error $e(t)$ is varied monotonically.

3.3 Stability and convergence analysis

Considering the error transformation (13) and defining $e_2(t) = \dot{\theta}_r - \omega$, the system (7) can be redescribed as

$$\begin{cases} \dot{\xi} = \frac{1}{\varphi}(e_2 - \dot{\varphi}\xi) \\ b\dot{e}_2 = b\ddot{\theta}_r + (v - u) - v(t) + a_1\theta + a_2\omega - a_3 + a_4\text{sgn}(\theta - \theta_0) + a_5\text{sgn}(\omega) - d(t) \end{cases} \quad (17)$$

Moreover, from (7) and (11), it follows $\tilde{d} = d - \hat{d} = b(\dot{\omega} - \dot{\hat{\omega}})$, then, $\tilde{d} = -\gamma\tilde{d} + \dot{\hat{d}}$, \tilde{d} exponentially converges to zero with a ratio determined by γ and the steady-state error depends on $\dot{\hat{d}}$. Accordingly, for the closed-loop system consisting of the system (17) and the designed controller (10)-(15), a candidate of the Lyapunov function is chosen as:

$$V = \frac{1}{2}\xi^2 + \frac{b}{2}z^2 + \frac{1}{2}\eta^2 + \frac{1}{2}\tilde{d}^2 \quad (18)$$

The time derivative of V is calculated as follows:

$$\begin{aligned} \dot{V} &= \xi \frac{1}{\varphi} (z + \alpha - \dot{\varphi} \xi) + z (b\dot{e}_2 - b\dot{\alpha}) + \eta \dot{\eta} + \tilde{d} (-\gamma \tilde{d} + \dot{d}) \\ &= -k_1 \xi^2 - k_2 z^2 - k_4 \eta^2 + z [(v-u) - k_3 (z-\eta)] - \gamma \tilde{d}^2 \\ &\quad - |zN(v-u)| - \frac{1}{2} (v-u)^2 + \eta (v-u) - z \tilde{d} + \tilde{d} \dot{d} \quad (19) \\ &\leq -k_1 \xi^2 - (k_2 - \frac{1}{2}) z^2 - (k_4 - \frac{1}{2}) \eta^2 - (\gamma - \frac{1}{2} - \frac{1}{2\epsilon}) \tilde{d}^2 \\ &\quad - [|zN(v-u)| - z(v-u)] - k_3 z (z-\eta) + \frac{\epsilon}{2} \dot{d}^2 \end{aligned}$$

where $\epsilon > 0$ is small enough. Nothing that $N > 1$ and $-k_3 z (z - \eta) \leq -\frac{1}{2} k_3 z^2 + \frac{1}{2} k_3 \eta^2$, then, (19) satisfies the following inequality.

$$\begin{aligned} \dot{V} &\leq -k_1 \xi^2 - (k_2 - 0.5 + 0.5k_3) z^2 - (k_4 - 0.5 - 0.5k_3) \eta^2 \\ &\quad - (\gamma - \frac{1}{2} - \frac{1}{2\epsilon}) \tilde{d}^2 + \frac{\epsilon}{2} \dot{d}^2 \quad (20) \end{aligned}$$

When choosing the adjustable parameters $k_1 > 0$, $k_2 > 0.5$, $k_3 > 0$, $k_4 > 0.5(1 + k_3)$, $\gamma > 0.5 + 1/(2\epsilon)$, it follows $\dot{V} < -\rho V + 0.5\epsilon \dot{d}^2$, $\forall (\xi, z, \eta, \tilde{d})$. Moreover, ϵ is small enough and for slow change of the unknown parameter perturbation, the disturbance input \dot{d} is almost to be zero. Therefore, the closed-loop control system is bounded-input bounded-output stable with the required static performance. Furthermore, due to $0 \leq \xi(t) < 1$ resulting from the transformation error $\xi(t) = e(t)/\varphi(t)$ and the definition of $\varphi(t)$, it follows that $e(t)$ can monotonically converges to zero and the whole response curve of $e(t)$ is limited to $0 \leq e(t) < \rho(t)$, $\forall t \geq 0$ if $e(0) > 0$ and $-\rho(t) < e(t) \leq 0$, $\forall t \geq 0$ if $e(0) < 0$, which means that there is no overshoot in the monotonically transient response of $e(t)$.

4. VERIFICATION OF SIMULATION AND EXPERIMENT TESTS

Firstly, using the model identified for real electronic throttle system as the controlled plant, the simulation results in Matlab/Simulink are given to validate the effectiveness of the proposed control strategy. Three typical operating cases are considered: the reference signal is set as step, ramp, and sinusoidal signals, respectively.

In simulation, considering the maximum of throttle valve opening $90[\text{deg}] = \pi/2[\text{rad}]$ and the required static precision and transient rapidity, the parameters of the prescribed performance function are chosen as $\rho_0 = 1.6$, $\rho_\infty = 0.02$, $\lambda = 60$. Meanwhile, according to the conditions (16), the adjustable parameters of the controller are selected as: $\gamma = 2000$, $k_1 = 40$, $k_2 = 10$, $k_3 = 10$, $k_4 = 10$, $N = 2$.

Note that in practice the valve angle of the electronic throttle is only measurable, thus, the feedback velocity ω in the controller is replaced by the estimate $\omega' = (\sigma s / (\beta s + 1)) \theta$, where s is the Laplace variable, β is a small number (chosen as 0.01) and the constant σ is a gain of the filter (chosen as 0.001) Pozo et al., (2009).

The simulation results are shown in Fig.6-Fig.8. It can be seen that in different reference signals, all the requirements are satisfied: the settling time about 55ms and no overshoot of the transient tracking performance; almost zero steady-state error; the control voltage within 12V; the throttle angle tracking error curve being between the upper and lower limits of the performance function.

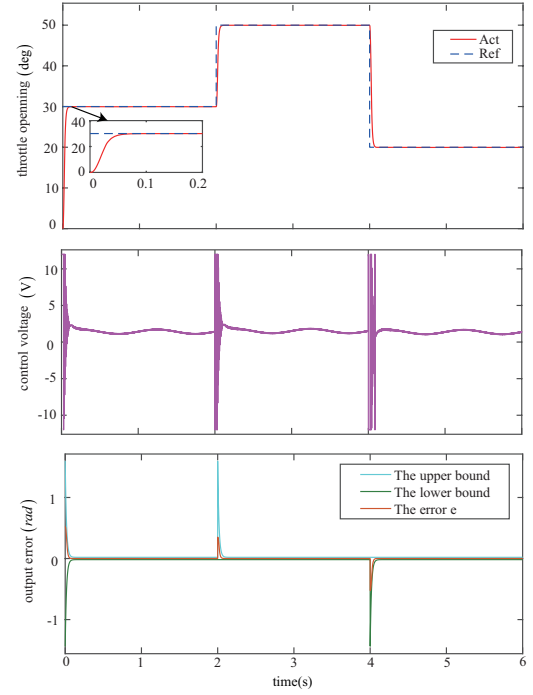


Fig. 6. Simulation result in step signal.

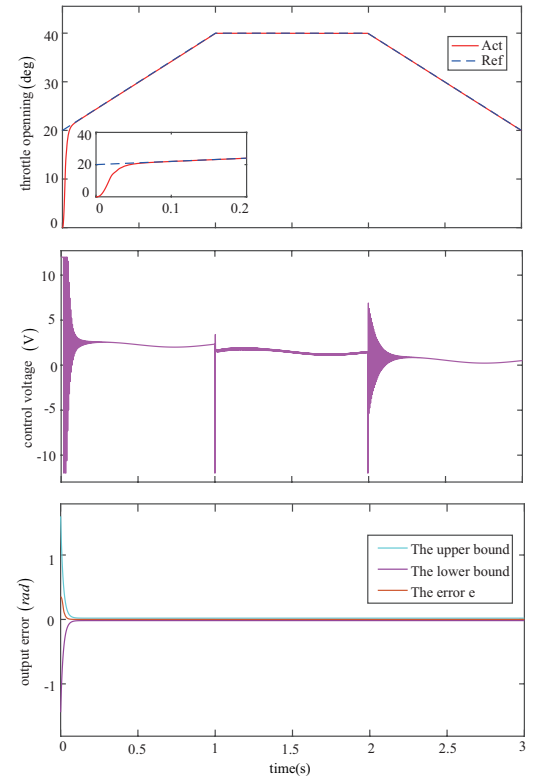


Fig. 7. Simulation result in ramp signal.

In order to show the superiority of the proposed prescribed performance servo control (PPSC) strategy, here the comparison with the finite-time servo control (FTSC) strategy in Li and Jiao, (2017) will be given. In simulation, the system model used is the same as that in Li and Jiao, (2017) and two cases, a combination of step signals and a periodical sinusoidal signals with small amplitudes nearby the LH position, are considered. The comparison

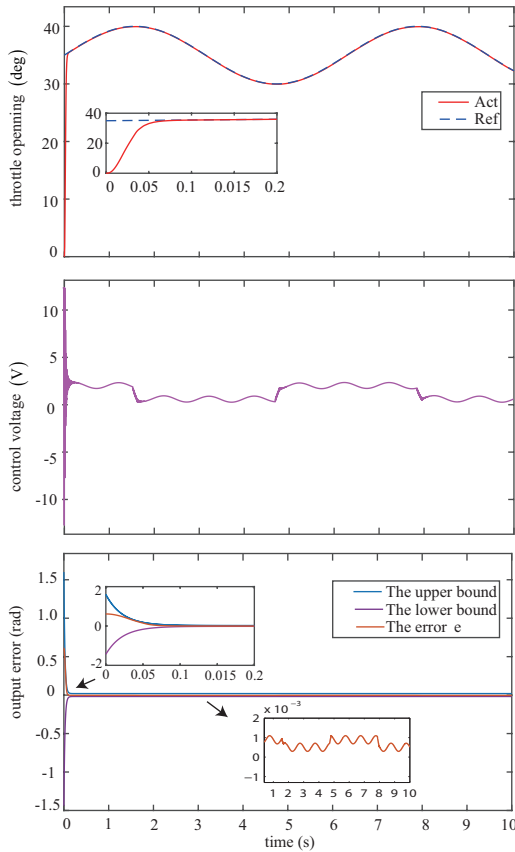


Fig. 8. Simulation result in sinusoidal signal

results are shown in Fig.9 and Fig.10. Obviously, it can be seen from Fig.9 and Fig.10 that both transient and static tracking performance of the proposed PPSC are superior to that of the FTSC, no overshoot, shorter settling time and almost zero steady-state error, in especial the tracking error curves of PPSC in the two cases are between the upper and lower limits of the performance function.

The designed controller is also implemented in the HIL experiment platform shown in Fig.3 to verify its applicability in practice. Without loss of generality, the two operating cases are considered:

Case 1. Step signals with large angle variation in very short time to validate the fast transient performance, shown in the dash line of Fig.11.

Case 2. Step signals with a small amplitude change to verify the steady state error overcoming the return springs, shown in the dash line of Fig.12.

Obviously, Fig.11 shows the settling time of the transient response about 55ms, both Fig.11 and Fig.12 show that no overshoot, the steady state error almost zero, and the tracking error curves in the two cases are between the upper and lower limits of the performance function.

In order to further show the superiority of the designed controller, HIL experimental comparison with Li and Jiao, (2017) is also given. First select the small angle of repeated step change as shown Fig.12 in Li and Jiao, (2017) as the expected signal, and the comparison result is shown in Fig.13. And then, the comparison result under a set of stair signals is shown in Fig.14. From both experimental

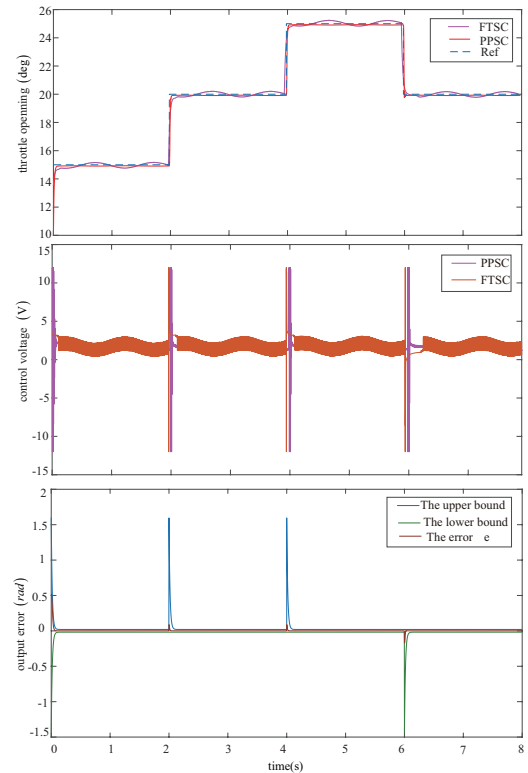


Fig. 9. Comparison result in simulation of Case 1

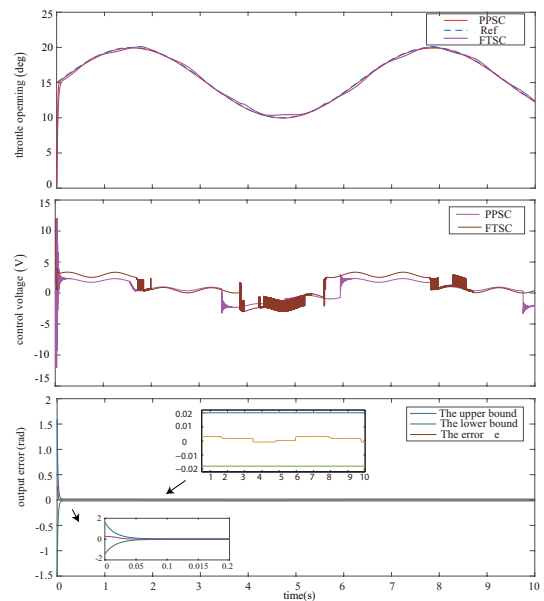


Fig. 10. Comparison result in simulation of Case 2

comparisons, it is further verified that the whole error curve of the proposed PPSC strategy is limited between the upper and lower limits of the performance function, and has better transient and static tracking response than the FTSC of Li and Jiao, (2017)—no overshoot and smaller steady-state error.

5. CONCLUSION

In this paper, a prescribed performance tracking controller of the throttle valve angle was designed and applied to

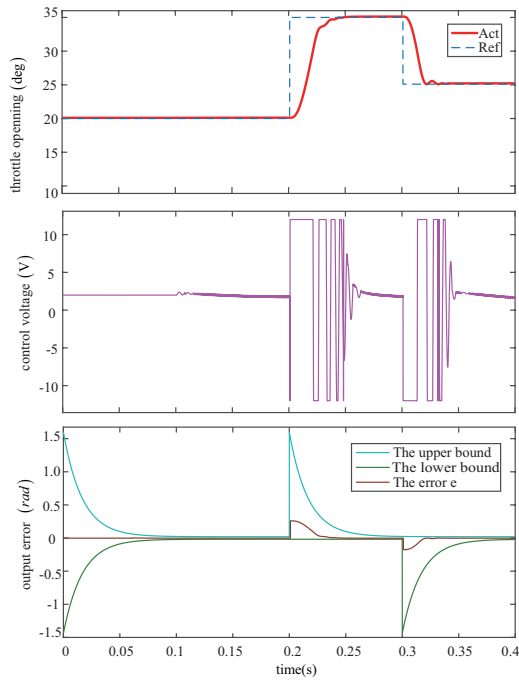


Fig. 11. Experimental result in Case 1.

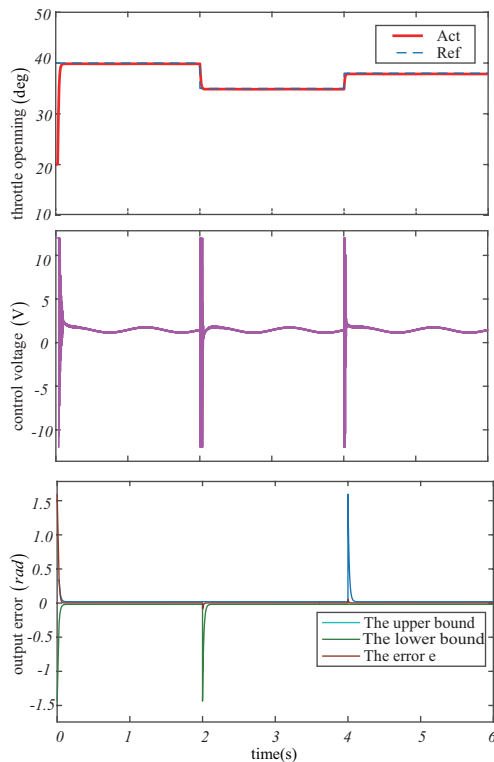


Fig. 12. Experimental result in Case 2.

a real automotive electronic throttle system. In the controller design, the system uncertainty and input saturation constraints were considered. The system uncertainty was handled through PSO identification for the nominal parameters and unknown input-observer-based estimate for the lumped disturbance including parameter perturbations and load torque disturbance. The input saturation was dealt with the auxiliary system design. Both simulation validations and experimental tests showed that the

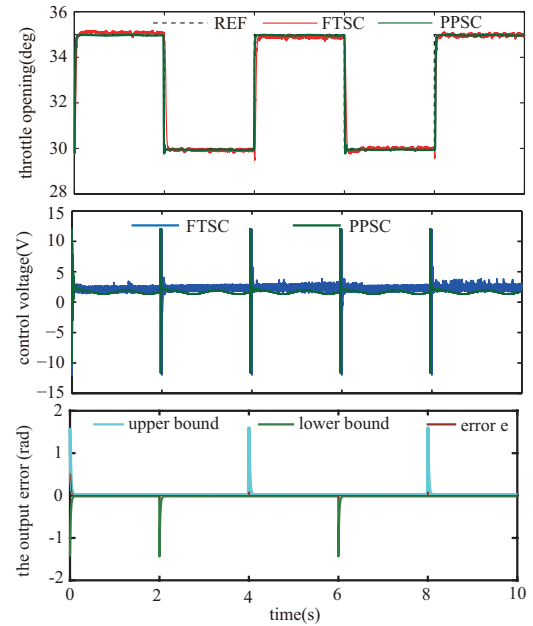


Fig. 13. Comparison in experiment under repeated steps.

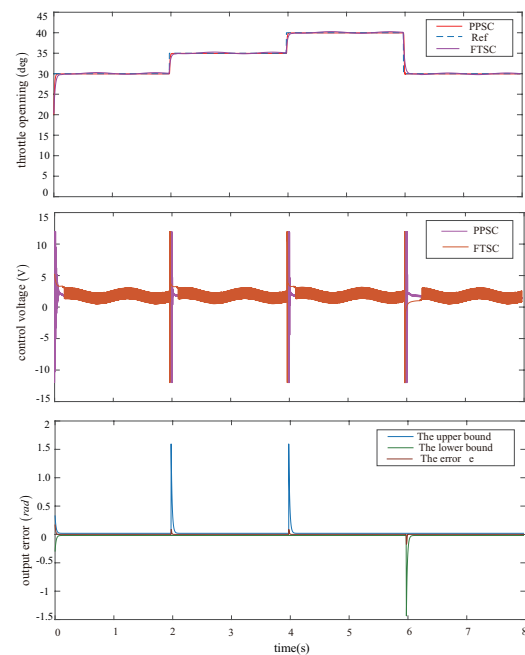


Fig. 14. Comparison in experiment under stair signals

utilization of the prescribed performance control technique ensures the shorter settling time with no overshoot and higher accuracy of steady state error through limiting the tracking error curve between the upper and lower limits of the prescribed performance function.

REFERENCES

- Alfi, A. (2011). PSO with adaptive mutation and inertia weight and its application in parameter estimation of dynamic systems. *ACTA Automatica Sinica*, 37(5):541–549.
- Bai, R. (2018). Adaptive sliding-mode control of automotive electronic throttle in the presence of input satu-

- ration constraint. *IEEE/CAA Journal of Automatica Sinica*, 5(4):878–884.
- Bechlioulis, C. P., and Rovithakis, G. A. (2009). Adaptive control with guaranteed transient and steady state tracking error bounds for strict feedback systems. *Automatica*, 45(2):532–538.
- Bernardo, M., Gaeta, A., Montanaro, U., and Santini, S. (2010). Synthesis and experimental validation of the novel LQ-NEMCSI adaptive strategy on an electronic throttle valve. *IEEE Trans. Control Syst. Technol.*, 18(6):1325–1337.
- Chen, M. M., Sam Ge, S. Z., and Ren, B. (2011). Adaptive tracking control of uncertain MIMO nonlinear systems with input constraints. *Automatica*, 47(3):452–465.
- Cook, A. J., Sun, J., and Buckland, J. H. (2006). Automotive powertrain control—a survey. *Asian Journal of Control*, 8(3):237–260.
- Corless, M., and Tu, J. (1998). State and input estimation for a class of uncertain systems. *Automatica*, 34(6):757–764.
- Deur, J., Pavkovic, D., and Peric, N. (2004). An electronic throttle control strategy including compensation of friction and limp-home effects. *IEEE Trans. Ind. Applications*, 40(3):821–834.
- Grepl, R., and Lee, B. (2010). Modeling, parameter estimation and nonlinear control of automotive electronic throttle using a rapid-control prototyping technique. *Int. Journal of Automotive Technology*, 11(4):601–610.
- Han, I. S., and Lee, J. M. (2013). Improved prescribed performance constraint control for a strict feedback nonlinear dynamic system. *IET Control Theory Applications*, 7(14):1818–1827.
- Jiao, X., Zhang, J., and Shen, T. (2014). An adaptive servo control strategy for automotive electronic throttle and experimental validation. *IEEE Trans. Ind. Electron.*, 61(11):6275–6284.
- Jiao, X., Li, G., and Wang, H. (2018). Adaptive finite time servo control for automotive electronic throttle with experimental analysis. *Mechatronics*, 53(4):192–201.
- Kennedy, J., and Eberhart, R. (1995). Particle swarm optimization. *Proceedings of 1995 IEEE International Conference on Neural Networks*, 1942–1948.
- Li, Y., Yang, H., and Yan, B. (2017). Extended state observer-based intelligent double integral sliding mode control of electronic throttle valve. *Advances in Mechanical Engineering*, 9(12):1–10.
- Li, G., and Jiao, X. (2017). Synthesis and validation of finite time servo control with PSO identification for automotive electronic throttle. *Nonlinear Dynamics*, 90(2):1165–1177.
- Li, Y., Yang, H., and Yang, B. (2018). An extended continuum model incorporating the electronic throttle dynamics for traffic flow. *Nonlinear Dynamics*, 93(4):1923–1931.
- Loh, R. N., Pornthanomwong, K. T., and Pyko, J. S. (2007). Modeling, parameters identification, and control of an electronic throttle control (ETC) system *International Conference on Intelligent and Advanced Systems*, 1029–1035.
- Na, J., Chen, Q., Ren, X., and Guo, Y. (2014). Adaptive prescribed performance motion control of servo mechanisms with friction compensation. *IEEE Trans. Ind. Electron.*, 61(1):486–494.
- Perez-Arancibia, N. O., Tsao, T. C., and Gibson, J. S. (2010). Saturation-induced instability and its avoidance in adaptive control of hard disk drives. *IEEE Trans. Control Syst. Technol.*, 18(2):368–382.
- Pozo, F., Acho, L., and Vidal, Y. (2009). Nonlinear adaptive tracking control of an electronic throttle system: Benchmark experiments. *IFAC workshop on engine and powertrain control, simulation and modeling*.
- Psomopoulou, E., Theodorakopoulos, A., Doulgeri, Z., and Rovithakis, G. A. (2015). Prescribed performance tracking of a variable stiffness actuated robot. *IEEE Trans. Control Syst. Technol.*, 23(5):1914–1926.
- Pujol, G., Vidal, Y., Acho, L., and Vargas, A. N. (2015). Asymmetric modelling and control of an electronic throttle. *Int. J. Numerical Modelling Electronic Networks Devices Fields*, 29(2):192–204.
- Sun, H., Zhao, H., and Huang, K. (2018). Nonlinear adaptive tracking control of an electronic throttle system: Benchmark experiments. *IEEE Trans. Fuzzy Syst.*, 26(2):694–704.
- Wang, C. H., and Huang, D. Y. (2013). A new intelligent fuzzy controller for nonlinear hysteretic electronic throttle in modern intelligent automobiles. *IEEE Trans. Ind. Electron.*, 60(6):2332–2345.
- Wang, W., Huang, J., and Wen, C. (2017). Prescribed performance bound-based adaptive path-following control of uncertain nonholonomic mobile robots. *Int. J. Adapt. Control Signal Process*, 31(5):805–822.
- Wang, H., Li, Z., and Jin, X. (2018a). Adaptive integral terminal sliding mode control for automobile electronic throttle via an uncertainty observer and experimental validation. *IEEE Trans. Veh. Technol.*, 67(9):8129–8143.
- Wang, H., Shi, L., and Man, Z. (2018b). Continuous fast nonsingular terminal sliding mode control of automotive electronic throttle systems using finite-time exact observer. *IEEE Trans. Ind. Electron.*, 65(9):7160–7172.
- Wen, C., Zhou, J., Liu, Z., and Su, H. (2011). Robust adaptive control of uncertain nonlinear systems in the presence of input saturation and external disturbance. *IEEE Trans. Automat. Control*, 56(7):1672–1678.
- Xue, J., Jiao, X., Sun, Z. (2018). ESO-based double closed loop servo control for automobile electronic throttle. *5th IFAC Conference on Engine and Powertrain Control, Simulation and Modeling, IFAC PapersOnLine*, 51-31: 979–983.
- Yang, B., Liu, M., Kim, H., and Cui, X. (2018). Continuous fast nonsingular terminal sliding mode control of automotive electronic throttle systems using finite-time exact observer. *Journal of Process Control*, 61(1):36–46.
- Yuan, X., Wang, Y., Sun, W., and Wu, L. (2010a). RBF networks-based adaptive inverse model control system for electronic throttle. *IEEE Trans. Control Syst. Technol.*, 18(3):750–756.
- Yuan, X., Wang, Y., and Wu, L. (2010b). Neural network based self-learning control strategy for electronic throttle valve. *IEEE Trans. Veh. Technol.*, 59(8):3757–3765.
- Zheng, Z., and Feroskhan, M. (2017). Path following of a surface vessel with prescribed performance in the presence of input saturation and external disturbances. *IEEE/ASME Trans. Mechatron.*, 22(6):2564–2575.